IOPscience iopscience.iop.org

Home Search Collections Journals About Contact us My IOPscience

Ion photostimulated desorption as a tool for investigating adsorption and electronic excitation of molecules on semiconductor surfaces

This article has been downloaded from IOPscience. Please scroll down to see the full text article.

2006 J. Phys.: Condens. Matter 18 S1461

(http://iopscience.iop.org/0953-8984/18/30/S06)

View the table of contents for this issue, or go to the journal homepage for more

Download details:
IP Address: 129.252.86.83
The article was downloaded on 28/05/2010 at 12:28

Please note that terms and conditions apply.

INSTITUTE OF PHYSICS PUBLISHING JOURNAL OF PHYSICS: CONDENSED MATTER

J. Phys.: Condens. Matter **18** (2006) S1461–S1478 doi:10.1088/0953-8984/18/30/S06

Ion photostimulated desorption as a tool for investigating adsorption and electronic excitation of molecules on semiconductor surfaces

Geneviève Comtet and Gérald Dujardin

Laboratoire de Photophysique Moléculaire, Bâtiment 210, Université de Paris-Sud, 91405 Orsay, France

Received 8 February 2006, in final form 20 March 2006
Published 14 July 2006
Online at stacks.iop.org/JPhysCM/18/S1461

Abstract

Ion photostimulated desorption (PSD) is a specific surface sensitive process. This paper reviews ion PSD following core level excitation of molecules adsorbed on the Si(111) 7 × 7 and Si(100) 2 × 1 surfaces. Several aspects of ion PSD will be discussed; (i) the use of ion PSD as a tool for investigating the adsorption configurations of O_2 on Si(111) 7 × 7, (ii) the relevance of ion PSD for probing the physisorption–chemisorption transition of benzene molecules on Si(111), (iii) the comparison between ion PSD of methanol adsorbed on Si(111) and photofragmentation of the methanol molecule in the gas phase, (iv) the comparison between ion PSD of formic acid adsorbed on the Si(111) and Si(100) surfaces and (v) the chemical selectivity of ion PSD following core level excitation of NO dissociatively adsorbed on Si(111). Finally, the interplay between ion dynamics and electronic relaxation following core level excitation and Auger processes will be discussed in the case of O^+ photodesorption from O_2 adsorbed on Si(111) 7×7, as investigated via isotope and temperature effects on both the intensities and kinetic energies of the desorbed ions.

1. Introduction

The adsorption and electronic excitation of molecules on semiconductor or insulating surfaces are key issues in molecular electronics for fabricating memories [1], organic light emitting diodes [2–4], thin film transistors [5, 6] and new materials [7]. The electronic excitation of adsorbates has also been proposed as a method for producing atomic scale structures on semiconductor surfaces [8]. The adsorption configurations of molecules on semiconductor surfaces have been extensively studied using valence band and core level electron photoemission [9] and near edge x-ray absorption fine structure [10]. Their electronic excitation and the subsequent dynamics have been studied to a lesser extent using ion photon stimulated desorption. The aim of this paper is to demonstrate that ion photon stimulated

 © 2006 IOP Publishing Ltd Printed in the UK

desorption is a powerful tool for investigating not only the adsorption but moreover the electronic excitation and the ensuing dynamics of adsorbed molecules on semiconductor surfaces.

Ion photon stimulated desorption (PSD) experiments on adsorbed atoms and molecules were first carried out in the early 1980s [11]. The substrates used were usually oxide and metal surfaces [12]. The understanding of the ion PSD mechanism was based on previous work on electron stimulated desorption [13]. Core level excitation was shown to produce more efficient ion photodesorption than inner valence excitation [14]. Ion PSD from semiconductor surfaces was first studied by Yarmoff *et al* [15] for fluorinated Si(111) surfaces, by measuring the desorbed ion yield and the photon absorption at the Si 2p edge. During the past 15 years, ion PSD of molecules [16–23], self-assembled monolayers [24–27] and thin films [28–32] on semiconductor surfaces have been extensively studied. In particular, ion PSD has been investigated by using coincidence techniques involving two photoions [33], and a valence or Auger electron and a photoion [34]. These studies, performed at the adsorbate core level thresholds, have enabled (i) the identification of the atomic sites responsible for ion desorption, (ii) the determination of the branching ratio between two desorption processes and (iii) the spectroscopic clarification of the ion desorption mechanism related to a specific Auger process.

In this paper, we review studies performed using photon excitation of both substrate or adsorbate core levels, where (i) the mass selected desorbed ion yields and photon absorption have been compared, (ii) the kinetic energy distribution of photodesorbed ions have been recorded and (iii) the valence band and XPS photoemission studies have been carried out simultaneously. The aim of this paper is to demonstrate that these studies have enabled (i) the investigation of the adsorption of molecules on semiconductor surfaces at low exposures, (ii) the comparison of gas phase photofragmentation and mechanisms of ion desorption and (iii) obtaining evidence of the interplay between ion dynamics and electron relaxation following core level excitation and Auger processes.

Section 2 gives a brief description of the experimental set-up, the different measurements performed on photodesorbed ions and photoemitted electrons, the preparation and characterization of the silicon surfaces, and the method used to adsorb molecules on surfaces and determine the surface coverage.

In section 3, we present ion photodesorption studies of the adsorption of O_2 on Si(111). Oxygen on silicon has emerged as a case study for the adsorption of small diatomic molecules on semiconductor surfaces due to the importance of growing thin oxide films in microelectronics [35–37]. Ion photodesorption, which is a very surface sensitive and site specific method, has been essential for probing the adsorption of O_2 molecules [38–40] as a function of the oxygen exposure and substrate temperature. Indeed, many different adsorption configurations have been evidenced [40]. Valence band photoemission study of O_2 adsorbed on Si(111) has been performed simultaneously and the correlation with O^+ ion PSD has enabled the assignment of the photoemission bands [40].

Section 4 underlines the interest of ion photodesorption and photoemission when studying the adsorption and the molecular dynamics of organic molecules, such as methanol [41–43], formic acid [44] and benzene [45, 46], on silicon surfaces. Comparison between ion photodesorption of adsorbed molecules and ion photofragmentation of gas phase molecules has revealed the role of the electronic coupling with the surface in the molecular dynamics [43]. Comparison between ion photodesorption of molecules adsorbed on the Si(111) and Si(100) surfaces has revealed different electronic couplings [44]. In the case of benzene on Si(111) 7×7, the transition from the physisorbed state to the chemisorbed one as a function of the substrate temperature has been characterized in both photoemission and ion photodesorption studies [45, 46].

Section 5 focuses on an important issue of the photodesorption processes, i.e. the direct or indirect character of the molecular electronic excitation. This is illustrated by the case of H^+ desorption from the hydrogenated diamond surface where direct and indirect electronic excitations are simultaneously observed [47, 48].

Section 6 discusses the ability to perform core level selective surface bond breaking as illustrated by the case of dissociatively adsorbed NO on the Si(111) 7 × 7 surface [49].

In section 7, we discuss the different steps of ion desorption following photon excitation. We consider in particular the electronic relaxation processes responsible for the recapture of the desorbing species. This has been investigated through the isotope and temperature dependence of the ion desorption yields and the kinetic energy of desorbed ions [50, 51].

2. Experimental details

All the experiments were performed at the storage ring Super-ACO of the synchrotron radiation facility in Orsay, using the SA23 beam line for photon excitation in the 30–160 eV range, and the SA72 beam line for photon excitation in the 150–800 eV range. The analysis chamber is an ultrahigh vacuum chamber with a base pressure of 2×10^{-11} Torr. It is equipped with a quadrupole ion spectrometer for ion detection, a cylindrical mirror analyser followed by a quadrupole mass spectrometer for mass selected ion kinetic energy measurements, and a hemispherical electrostatic analyser for electron photoemission measurements. All the detectors are in a fixed position. Ions are detected at 45° from the photon beam. Electrons are detected at 90° from the photon beam. The sample is vertical and mounted on a specially designed sample holder, which allows the impinging angle of the photon beam on the surface to be modified. The sample holder can cool the sample down to 30 K by using a liquid helium flow cryostat, and can heat the sample up to 1500 K by direct resistive heating.

Different types of measurement have been performed:

(i) The number of secondary electrons has been recorded as a function of the photon energy scanned around the adsorbate or substrate core level ionization energies. This is usually called the near edge x-ray absorption fine structure (NEXAFS) spectrum. In this paper, this will be called the NEXAFS of electrons.
(ii) Similar spectra were recorded by detecting mass selected desorbed ions instead of secondary electrons. This will be called the NEXAFS of ions.
(iii) The number of photoelectrons has been recorded as a function of their kinetic energy at a fixed photon energy of about 40 eV (valence band photoemission spectrum).
(iv) The number of mass selected desorbed ions has been recorded as a function of their kinetic energy at a fixed photon energy. This will be called the kinetic energy distribution (KED) of mass selected ions.

The surface preparations were performed as follows. Both the Si(111) and the Si(100) samples were n-type, phosphorus doped with 1 and 5 Ω cm resistivity, respectively. First, they were outgassed for at least 12 h by resistive heating at 700 °C (Si(111)) and 600 °C (Si(100)) in the UHV (ultrahigh vacuum) chamber. The pressure during the last 3 h of the outgassing was less than 8×10^{-11} mbar. The clean reconstructed Si(111) 7 × 7 surface was then prepared by several 30 s flashes at 1100 °C. The clean reconstructed Si(100) 2 × 1 surface was prepared by a few minutes' heating at 900 °C, followed by several 30 s flashes at 1100 °C. For both surfaces, the pressure during the last flashes was less than 1×10^{-10} mbar. The quality of the surface reconstruction was checked through the observation of the surface states in the electron UV photoemission spectra.

The base pressure in the UHV chamber is typically 2×10^{-11} mbar. Each molecular deposition was performed by increasing the pressure up to 1×10^{-9} mbar, and keeping the pressure constant for a time depending on the sticking coefficient of the molecule and the expected coverage of the surface. The exposures were corrected for the sensitivity factor of each molecule with respect to nitrogen for which the Bayer–Alpert ion gauge is calibrated. The surface coverage was deduced from the decrease of the silicon surface states observed in valence band photoemission spectra. Our experimental set-up, where the electrons are detected at 90° from the photon beam, allows a very sensitive observation of the surface states of both the Si(111) 7×7 and Si(100) 2×1 surfaces. The surface coverage was deduced from the partial saturation of the adatom and/or the restatom surface states of the Si(111) 7×7 surface and of the dimer surface states of the Si(100) 2×1 surface.

An important problem, which may arise in synchrotron radiation experiments, is the modification of the adsorbate or the surface due to photoinduced reactions. In all the reported experiments, the photon illumination of the surface (typically 10^{13} photons s^{-1} cm^{-2}) was low enough to avoid any sample modification. This has been verified by recording the time evolution of both the ion desorption signals and the intensities of surface state bands in photoemission. The stability of these signals over the duration of the experiment (typically a few hours) indicated that neither the adsorbed molecules nor the surface were significantly modified by the photon irradiation.

3. Combined ion photodesorption and electron photoemission studies of O_2 on Si(111) 7×7

The adsorption of molecular oxygen on the Si(111) 7×7 surface is a complex process, and has given rise to a large number of studies with contradictory results [52–55]. The main difficulty is that this adsorption depends critically on the substrate temperature and on the amount of oxygen exposure. We show here how ion PSD has provided evidence of different adsorption configurations of O_2 on the Si(111) surface and information on their electronic structure in combination with valence band photoemission.

Photon excitation in the 90–130 eV energy range of the Si(111) surface exposed to O_2 is followed by O^+ desorption. NEXAFS of O^+ ions have been recorded for different O_2 exposures on the silicon surface at 300 and 30 K, respectively [40]. Various forms of spectra shapes have been obtained (see figure 1), that are either similar to the NEXAFS of electrons with a step edge at 100 eV, or include essentially two resonances at 108 and 115 eV. Sometimes, the spectra include in various proportions both the step edge at 100 eV and the two resonances at 108 and 115 eV [40]. This indicates the presence of at least two different adsorption configurations of O_2 on Si(111), one giving rise to an indirect O^+ photodesorption process and the other one giving rise to two resonant O^+ photodesorption processes. The first adsorption configuration is present alone on the surface at 30 K for exposures below 0.02 L, and then coexists with a second one for exposures up to 0.09 L. The second adsorption configuration is predominant for exposures higher than 0.09 L at 30 K, and whatever the exposure is at 300 K. To find out whether the observed O^+ photodesorbed ion originates from the adsorption of one or two molecules on the same initial site, the O^+ yield has been recorded as a function of the O_2 exposure at the nominal photon excitation energy of 108 eV (see figure 2). At 300 K, the O^+ desorption yield first increases quadratically and then saturates (see figure 2(a)). This exposure dependence indicates that the O^+ photodesorbed ions originates from double adsorption configurations (two O_2 molecules have successively reacted on the same silicon site), and the number of available adsorption sites is limited. At 30 K, the exposure dependence is more complicated (figure 2(b)) [40]. As the O_2 exposure is increased, the O^+ yield first increases linearly up to

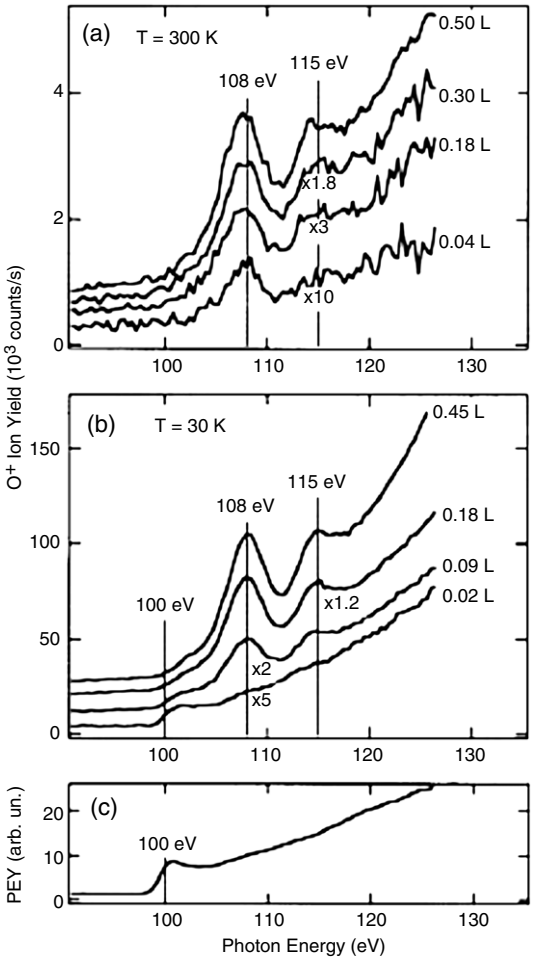

Figure 1. NEXAFS of O^+ ions around the Si 2p threshold energy (a) for O_2 exposures of 0.04, 0.18, 0.3 and 0.50 L on the Si(111) 7 × 7 surface at 300 K and (b) for O_2 exposures of 0.02, 0.09, 0.18 and 0.45 L on the Si(111) 7 × 7 surface at 30 K. All the curves have been normalized to the same photon flux. Curve (c) is the NEXAFS of secondary electrons in the same photon energy range and with the same photon energy resolution (1 eV) [40].

0.02 L. Then the yield somewhat saturates again above 0.1 L. Finally, the yield increases rapidly up to 0.4 L. The major difference between the 300 K (figure 2(a)) and 30 K (figure 2(b)) O^+ ion yield curves is observed in the low exposure (<0.02 L) regime. The O^+ ion yield curve at 300 K can be fitted by a quadratic function (see figure 2(a)) since its derivative always increases in the 0–0.02 L range. In contrast, the O^+ ion yield curve at 30 K can be fitted by a linear function (see figure 2(b)) since its derivative is constant and even decreases in the 0–0.02 L range. The linear increase of the O^+ yield curve up to 0.02 L indicates that the O^+ yield arises from single adsorption configurations. The behaviour of the O^+ yield above 0.4 L may not be associated with single or double adsorption configurations but rather with a mixture of single and double adsorption configurations having different photodesorption cross-sections. From this study, it appears that single adsorption sites at 300 K are not detected through O^+ photodesorption. This implies that the corresponding adsorbed O_2 molecules are dissociated

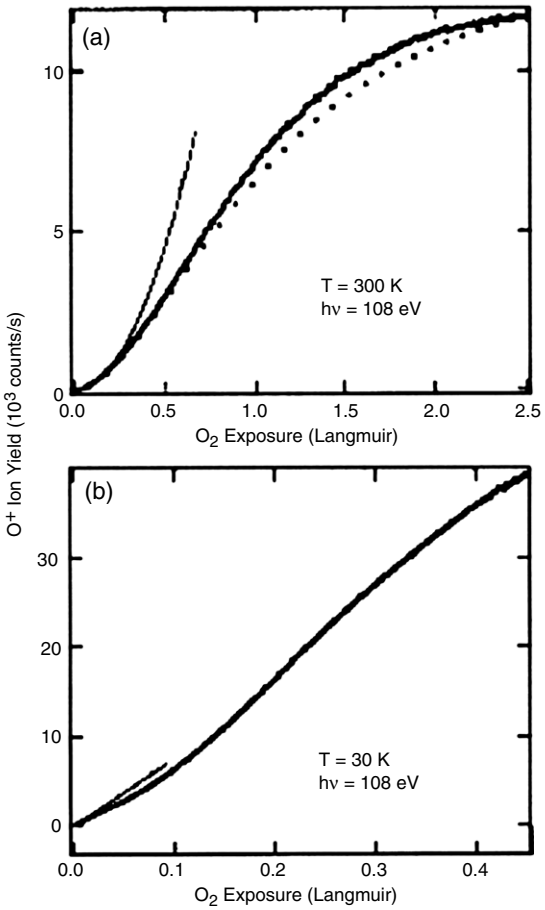

Figure 2. O^+ ion desorption yields recorded as a function of the O_2 exposure on the Si(111) 7×7 surface at 300 K (a) and at 30 K (b) and normalized to the same photon flux. The photon energy is 108 eV [40].

and that the oxygen atoms are in the Si back bonds [40]. These single adsorption sites are called 'ins–ins' configurations (ins for inserted) (figure 3(b)). In contrast, at 30 K, single adsorption sites give rise to O^+ photodesorption. It follows that they have at least one oxygen atom in the 'ad' position (they are called 'ad–ad' and 'ad–ins' configurations; figure 3(a)). The double adsorption configurations, observed both at 30 and 300 K, are characterized by a resonant excitation process at 108 and 115 eV. These resonances have been assigned to transitions from Si 2p core levels to the t_2 (3p) and $e(\varepsilon d)$ unoccupied molecular orbitals of SiO_4^- clusters in silicon dioxide [56]. This suggests that the double adsorption configurations giving rise to the O^+ photodesorption have an atomic arrangement similar to the tetrahedral oxygen arrangement in silicon dioxide, i.e. a silicon atom surrounded by four oxygen atoms, the so-called 'ad–insx3' configuration (figure 3(c)).

Valence band photoemission studies (photon energy 37 eV) have been performed simultaneously under the same temperature and exposure conditions [40]. Each photoemission band intensity was recorded as a function of O_2 exposure (figure 4), and linear or quadratic behaviours were observed depending on the temperature and the amount of oxygen. It was

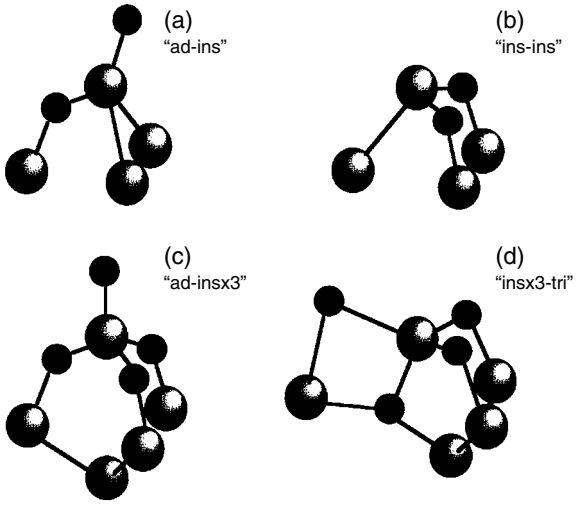

Figure 3. Most probable adsorption configurations of O_2 on Si(111) 7 × 7. A single O_2 molecule has reacted with a silicon adatom site ((a) and (b)). Two O_2 molecules have successively reacted on the same silicon adatom site ((c) and (d)). The large and small circles represent Si and O atoms, respectively [55].

concluded that each photoemission band should be associated with a specific bond rather than with a specific adsorption configuration. Finally, by comparing the exposure dependence at 300 and 30 K of the intensities of the two main photoemission bands and of the O^+ yield, the existence of 'insx3-tri' double adsorption configurations (see figure 3(d)) at 300 K was deduced.

In summary, ion PSD [40] has evidenced single and double adsorption configurations of O_2 adsorbed on Si(111) 7×7, depending on the substrate temperature and the O_2 exposure. The single adsorption configurations are found to be different at 300 K (ins–ins configuration) and 30 K (ad–ins or ad–ad configurations). The double adsorption configurations are essentially 'ad–insx3' at 30 K, while both 'ad–insx3' and 'insx3-tri' coexist at 300 K, as deduced from the comparison of the O_2 exposure dependence of the O^+ ion yield with the photoemission band intensities. The same methodology of combining ion PSD and valence band photoemission has been applied to investigate other molecular adsorption processes on silicon surfaces. In the case of the adsorption of O_2 on Si(100) 2 × 1, the presence of an oxygen precursor at 50 K, which does not exist at 300 K, has been evidenced [57]. In the case of the adsorption of NO on Si(111) 7 × 7, the three types of adsorption configuration evidenced by photoemission have also been seen using ion PSD [49]. In the case of NO on Si(100) 2 × 1 [58], the observation of O^+ photodesorbed ions around the Si 2p threshold and the lack of any observation of N^+ ions demonstrated that migration of nitrogen occurs in the subsurface region. The different patterns of O^+ photodesorption in the O 1s energy range showed that the partial subsurface migration of oxygen is more efficient at room temperature than at low temperature [58].

4. Combined ion photodesorption and electron photoemission studies of organic molecules on silicon surfaces

We wish to illustrate here the interest of ion photodesorption and photoemission when studying the adsorption and the molecular dynamics of small organic molecules on silicon surfaces.

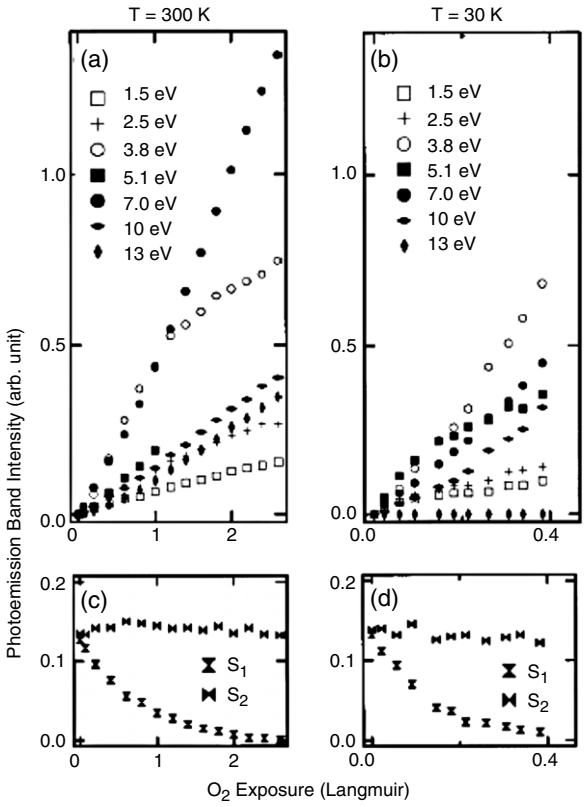

Figure 4. O_2 exposure dependences of the intensities of seven oxygen induced bands ((a) and (b)) and of the S_1 and S_2 bands ((c) and (d)) in the electron photoemission spectra of O_2 on Si(111) 7×7 at 300 K ((a) and (c)) and 30 K ((b) and (d)). All the intensities have been normalized to the same photon flux [40].

Deuterated molecules have been used instead of hydrogenated ones, as reliable data cannot be obtained from the H^+ ion. Indeed, due to their low mass, H^+ ions are very efficiently photodesorbed and a H^+ ion PSD signal is commonly present from clean silicon surfaces even before any deposition of the molecules.

We will first discuss the comparison between ion PSD of adsorbed deuterated methanol and the ionic fragmentation of methanol in the gas phase. It has been shown that the delocalization of the initial electronic excitation following the photoexcitation of gas phase methanol does not take place for the adsorbed molecule [43]. The adsorption of methanol on Si(111) 7×7, as studied using valence band photoemission [41], is dissociative and occurs via σ_{O-D} bond breakage and σ_{Si-O} formation. Ion PSD experiments of the methoxy species [43] have been performed in the exposure regime where all the Si restatoms are saturated and the Si adatoms are partly saturated. At the C 1s threshold, several positively charged fragments are produced through resonant mechanisms, C^+, CD^+ CD_2^+ and CD_3^+ at a 288 eV photon energy and D^+ at a 290 eV photon energy. The photoexcitation of methanol in the gas phase produces the same series of ionic fragments, but all of them are resonantly produced at both 288 and 290 eV photon excitation energies [43]. From this comparison, the 288 and 290 eV resonances are assigned to a transition of a C 1s electron to a molecular antibonding orbital mainly localized on the C–O bond and the C–H bond (C–D bond for adsorbed methanol), respectively. Following the

photoexcitation of the C–O bond (C–H bond) of methanol in the gas phase, both H^+ and CH_x^+ fragments are produced. On the other hand, following the photoexcitation of the C–O bond (C–D bond) of adsorbed methanol, only CH_x^+ ions (H^+ ions) are produced. It was deduced that the electronic coupling of the methoxy species with the surface suppresses the delocalization of the initial electronic excitation, which was possible in photoexcited gas phase molecules [43].

We report now on the capability of ion PSD for investigating the different couplings of deuterated formic acid with the semiconducting Si(100) 2×1 and the metallic Si(111) 7×7 surfaces [44]. Upon adsorption on Si(100) 2×1 and Si(111) 7×7, formic acid dissociates into an unidentate formate and an H atom [59]. In the case of deuterated formic acid on Si(100), following excitation at the C 1s threshold, four positively charged ions, D^+, CD^+, O^+ and CDO^+, are resonantly produced at energies of 288 and 292 eV. However, in the case of deuterated formic acid on Si(111) 7×7, following excitation at the C 1s threshold, only two ions are resonantly produced, namely D^+ ions at both 288 and 292 eV photon energies, and CDO^+ ions at 288 eV photon energy. The 288 and 292 eV resonance energies, also observed in the NEXAFS of electrons of formic acid on both surfaces, have been assigned to the excitation of C 1s electrons to the $\pi^*_{(C=O)}$ and $\sigma^*_{(C-D)}$ resonances, respectively [60]. It appears that the excitation of the π^*(C=O) resonance produces four positively charged ions when formic acid is adsorbed on the Si(100) surface, and only one ion from the Si(111) surface. However, excitation of the σ^*(C–D) resonance produces four positively charged ions for formic acid adsorbed on the Si(100) surface and no positively charged ion for formic acid on the Si(111) surface. Therefore, ion PSD following excitations at the C 1s threshold gives evidence that the Si(111) 7×7 surface more efficiently quenches the electronic excitation of the different orbitals of the adsorbed formic acid and prevents their delocalization. Similar conclusions have been obtained from ion PSD at the O 1s threshold [44]. This illustrates the ability of ion PSD to compare the coupling of a molecule with various surfaces.

Finally, we underline the interest of ion PSD for probing the physisorption–chemisorption transition in the case of deuterated benzene molecules adsorbed on Si(111) 7×7 [23]. The transition of benzene molecules from a physisorbed state to a chemisorbed was characterized first by valence band electron photoemission [45, 61]. Following the adsorption of 0.15 L of benzene on Si(111) at 30 K, the bands associated with the silicon surface states are not affected, while the adsorption features are very intense and show a one to one correspondence with the gas phase features indicating that benzene is physisorbed. When benzene molecules are adsorbed on Si(111) at 300 K, the intensity of the bands associated with silicon surface states is quenched and the features related to the degenerate orbitals of benzene are split, showing that benzene is chemisorbed. Upon increasing the temperature of a silicon surface exposed to 0.15 L of benzene at 30 K, the adsorption features gradually change from degenerate to non-degenerate, with a physisorption to chemisorption transition in the 75–105 K range. This transition from a physisorbed state to a chemisorbed state of benzene has also been determined by ion PSD [46]. The NEXAFS of D^+ ions, at the C 1s excitation threshold, is structured for physisorbed benzene and structureless for chemisorbed benzene. Therefore, the NEXAFS of D^+ ions is a signature of the physisorbed or chemisorbed state of benzene on Si(111). After various benzene exposures at 30 K, the D^+ ion yield and C 1s photoelectron yield have been recorded while increasing the substrate temperature. While the C 1s photoelectron yield stays constant as a function of temperature, indicating that no benzene desorption occurs, all the D^+ ion yield curves show a drop starting at 110 K for a 0.1 L exposure and in the 130–140 K range for higher benzene exposures (figure 5). The NEXAFS of D^+ ions, recorded before and after the drop in the D^+ ion yield curve, shows that the physisorption–chemisorption transition has occurred (figure 5). The transition temperature has been deduced to be around 110 K [46]. This transition temperature is 30 K higher than the one measured from valence

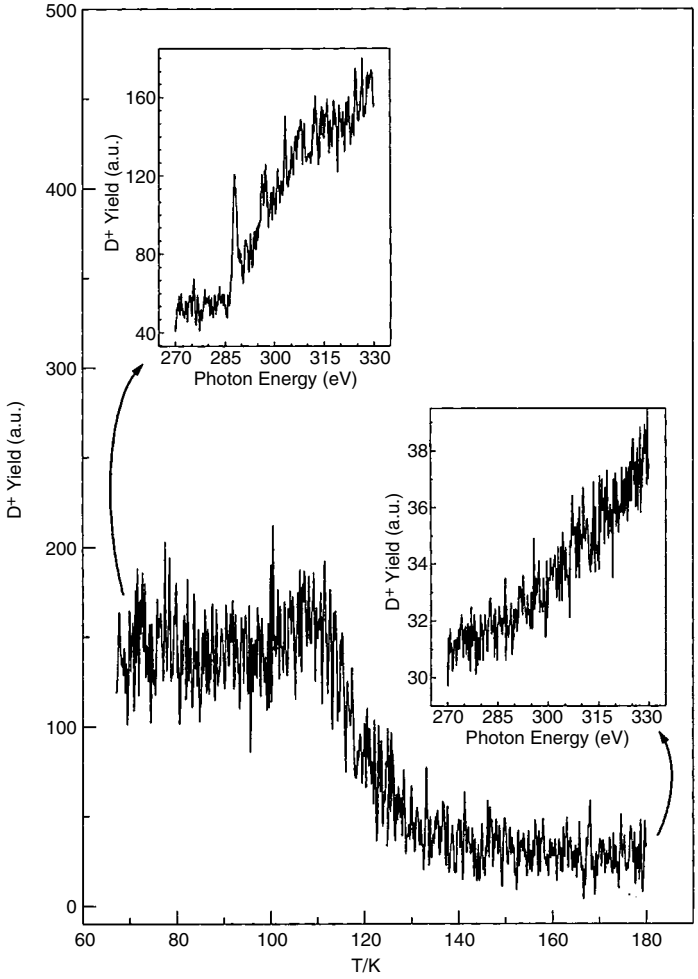

Figure 5. Photoexcitation spectra of 0.1 L benzene on Si(111) 7 × 7 at the beginning of the experiment, i.e. at 67 K, and at the end, i.e. at 180 K. The two spectra are significantly different in terms of ion yield and spectral structure, showing two different benzene adsorption states [46].

band photoemission [45]. This is due to a better measurement of the temperature, directly on the back of the silicon sample, in the case of the ion PSD experiments. This illustrates the ability of ion PSD to determine physisorption to chemisorption transition temperatures.

5. Direct and indirect ion photodesorption following core excitation

A key problem in ion photodesorption processes induced by core level excitation is to distinguish between direct and indirect processes. Direct processes require that the photon excitation, the relaxation of core holes and the ion desorption all occur around the same atomic site. In contrast, indirect processes are those induced by secondary electrons. In this case, the photon excitation in the bulk and the ion desorption occur at distinctly different atomic sites. The relative contribution of direct and indirect processes may be studied by comparing the NEXAFS of ions and the NEXAFS of secondary electrons. This is best illustrated in the

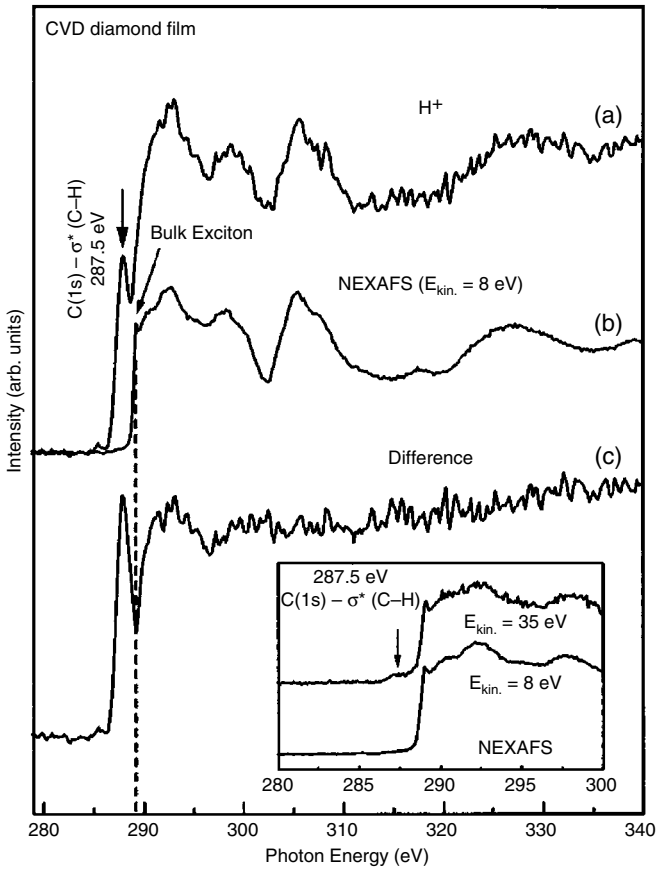

Figure 6. NEXAFS of H^+ ions around the C 1s threshold energy from a CVD diamond film (curve (a)) compared to the NEXAFS of secondary electrons (curve (b)). Curve (c) is the difference between the NEXAFS of H^+ ions and the normalized NEXAFS of secondary electrons. In the inset the NEXAFS of 8 and 35 eV secondary electrons (bulk and surface sensitive modes, respectively) are shown [48].

case of photon stimulated H^+ ion desorption from a hydrogenated CVD diamond film [48]. The NEXAFS of secondary electrons (figure 6(b)) displays features above the C 1s ionization threshold, which mainly correspond to bulk ionization processes. The NEXAFS of H^+ ions (figure 6(a)) displays similar features plus a sharp resonance at 287.5 eV, i.e. 2 eV lower than the threshold of the NEXAFS of secondary electrons. This resonance has been assigned to the electronic photon excitation of the C 1s electron to the antibonding σ^* orbital of the surface C–H bond. The features above the C 1s ionization threshold in the ion NEXAFS spectrum (figure 6(a)) correspond to indirect H^+ ion desorption. In contrast, the resonant feature at 287.5 eV corresponds to a direct H^+ ion desorption. This illustrates the intrinsic surface sensitivity of ion photon stimulated desorption.

6. Chemical selectivity of ion photodesorption following core excitation

The chemical selectivity of photon excitation of core levels is easy to realize since the core levels of two chemically different atoms have different energies. The subsequent chemical

selectivity of ion photodesorption processes is less straightforward, since it implies that the bond breaking occurs at the chemically selected atomic sites. In section 5, we have discussed the direct and indirect ion photodesorption processes following core excitation. Indirect processes cannot be chemically selective, since the secondary electrons responsible for the ion desorption have no memory of the initially excited core level. Direct processes may be chemically selective. This selectivity could be used to desorb a specific surface atom and pattern atomic scale structures, provided the surface has some initially adequate reconstruction [8].

We review here studies on the chemical selectivity of ion PSD following N(1s) and O(1s) core level excitations of the heteronuclear NO molecule, adsorbed on the Si(111) 7 × 7 surface [49]. Combined valence band photoemission and PSD at the Si 2p core level have shown that the adsorption of NO is dissociative and that SiN_xO_y species are produced on the surface [49]. The objective was to investigate whether the core level excitation of N 1s (O 1s) selectively produces the desorption of N^+ (O^+) ions. In fact, the N^+ ion intensity was always found to be less than 1% of the O^+ intensity. The reason is that, although N^+ is lighter than O^+ and is expected to leave the surface more rapidly, the nitrogen atom in the SiN_xO_y species is bound to three silicon atoms whereas the oxygen atom is expected to be bound to only one or two silicon atoms. Despite the absence of N^+ desorption, the selectivity of ion desorption was tested by comparing the O^+ ion desorption after O 1s and N 1s core excitation. As seen in figures 7(a) and (b), the O^+ ion yield shows various resonance features around the O(1s) threshold energy whereas no feature is seen around the N 1s threshold energy. This indicates that O^+ ion desorption can be achieved selectively by core excitation.

For multilayers of NO condensed on Si(111) 7 × 7, both O^+ and N^+ ions could be detected after N 1s and O 1s excitations. Around the N 1s ionization energy, the N^+ yield shows an increase as a function of photon energy and several resonances, while the O^+ yield slowly decreases and shows no resonance (figure 7(c)). The opposite result is found around the O 1s ionization energy (figure 7(d)), since the O^+ yield curve increases as a function of the photon energy and shows resonances whereas the N^+ ion yield curve shows no variation in intensity over the same photon energy range. Although the situation is very different here compared to that for NO molecules dissociatively chemisorbed on Si(111) 7 × 7, selective core level ion desorption is also observed for condensed NO molecules [49].

7. Ion photodesorption mechanisms

In this section, we shall investigate in more detail the ion photodesorption mechanisms following direct core level excitation. After core level excitation of the adsorbate or substrate surface atoms, a rapid Auger relaxation takes place leaving the adsorbate species in various ionic states [62]. The conversion of the electronic energy of these ionic states into the kinetic energy of the desorbing ions can be understood from the semiclassical MGR model [62], where the atom dynamics is treated classically and the electronic relaxations as quantum transitions between electronic states. The key point of this model is the competition between the molecular dynamics of the ionic states (leading to the ion desorption) and their relaxation and/or neutralization by electronic coupling with the substrate. A detailed description of these mechanisms is far from being possible. However, as it will be seen below, interesting insights can be obtained by measuring both the yield of desorbed ions and their kinetic energies, and by varying the balance between molecular dynamics and electronic relaxation, with isotope and temperature effects.

The best investigation of such ion photodesorption mechanisms has been the case of O^+ ion desorption from oxygen on Si(111) 7 × 7 [50, 51]. These studies were performed by resonant photon excitation at 108 eV (Si 2p core excitation) of the double adsorption configuration of

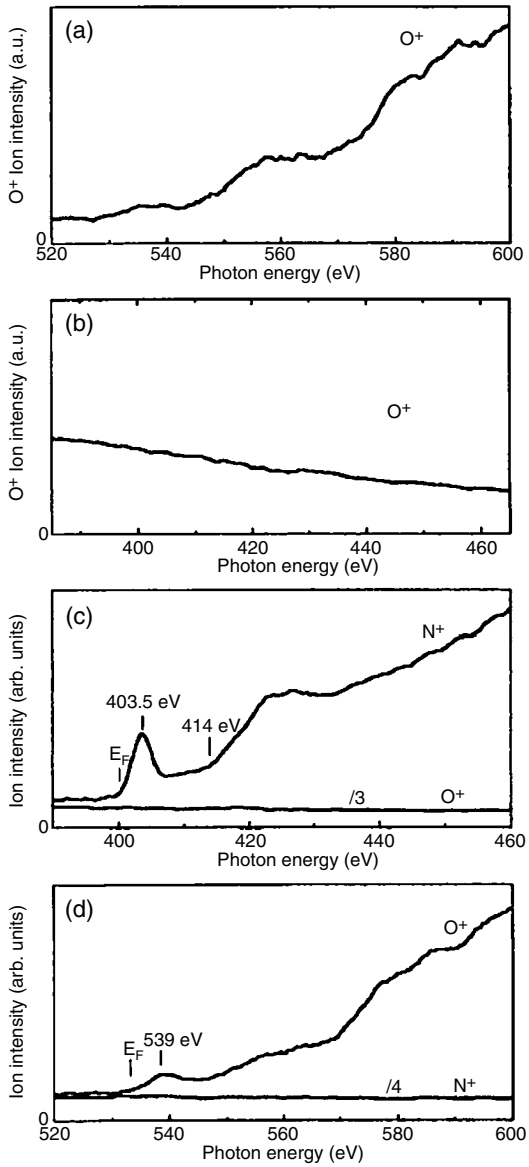

Figure 7. (a) NEXAFS of O^+ ions around the O 1s threshold energy after an exposure of Si(111) 7×7 to 3.5 L of NO at 320 K. (b) Same as (a), but around the N 1s threshold energy. (c) Relative NEXAFS of N^+ and O^+ around the N 1s threshold energy after an exposure of the Si(111) 7×7 surface to 3.2 L of NO at 21 K. (d) Same as (c) but around the O 1s threshold energy [49].

oxygen (see section 1). The balance between the ion dynamics and electron relaxation was varied by using oxygen isotopes [51], and different substrate temperatures [50].

By varying the oxygen isotope (^{18}O versus ^{16}O), the dynamics of the ion desorption can be modified. Indeed, the heaviest isotope ion ($^{18}O^+$) should stay longer in the vicinity of the surface, thus increasing the role of the electronic relaxation by the surface. The ratio of the total $^{18}O^+$ and $^{16}O^+$ yields was found to be 0.67 ± 0.02 [51]. Starting from the simplest

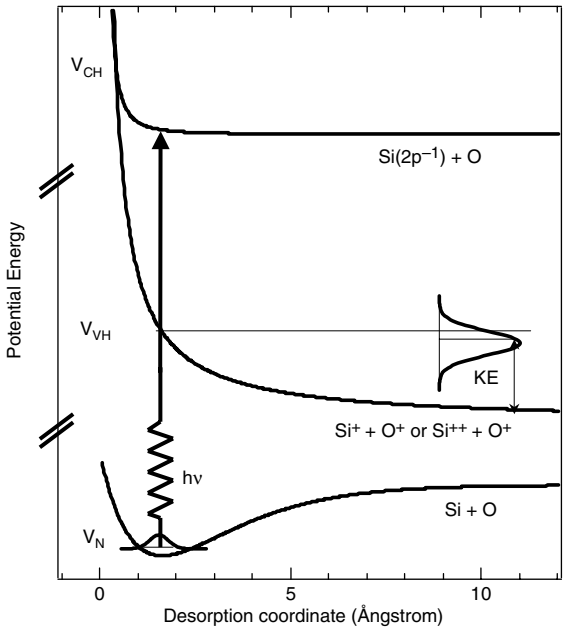

Figure 8. Potential energy curves involved in the three step model of photodesorption of O^+ from O_2 adsorbed on Si(111) 7 × 7. V_{CH} is the neutral core excited state, V_{VH} is a valence hole excited state and V_N is the ground state [51].

MGR-type model [62], the model shown in figure 8 was proposed. From this, an O^+ escape probability of 1.3×10^{-3} was deduced [51]. The escape probability is the probability for an O^+ ion, initially at the distance R_0, to escape along the $V_{VH}(R)$ potential energy curve before any relaxation to the $V_N(R)$ neutral ground state can occur. As shown in [51], this has enabled a value to be deduced of about 2 fs for the relaxation time, $\tau_{VH}(R_0)$, of the ionic species in the V_{VH} state. In fact, it has been shown that this model is oversimplified in accounting for further measurements of the isotope effect on the O^+ ion kinetic energy [51]. Indeed, such a surprising isotope effect on the kinetic energy could be explained only within a more complicated model (figure 9) involving two separate dissociative electronic states having different relaxation lifetimes of about 40 and 0.5 fs [51]. Although the model in figure 9 is only schematic, these results suggest that the relaxation lifetimes of the electronic excited states are very short, of the order of the femtosecond. Furthermore, this demonstrates that complex desorption mechanisms involving a cascade of electronic relaxations from several dissociative electronic states need to be considered to fully explain the observed isotope effects.

By varying the temperature of the silicon substrate, the electronic relaxation can be modified. Indeed, the temperature is expected to affect (i) the coupling with the substrate phonons, (ii) the charge carrier densities, (iii) the thermal contraction of the substrate and (iv) the thermally activated processes. Detailed information has been obtained by analysing the O^+ ion kinetic energy distributions (KED) at 300 and 30 K [50]. As shown in figure 10, the overall O^+ ion intensity is greater at 30 K than at 300 K. Moreover, the ion KED are different. In particular, the relative intensities of the two bands at 4 and 10 eV in the ion KED have changed. The intensities of the 4 and 10 eV bands increased by factors of 3.4 and 1.7, respectively, when the temperature was lowered from 300 to 30 K. These results were ascribed to a lengthening of the relaxation lifetimes of the ionic electronic states producing the O^+ desorbed ions [50]. This

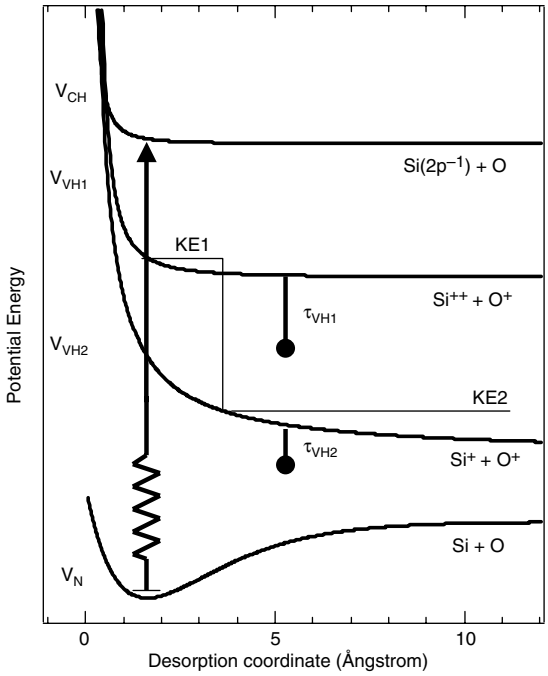

Figure 9. Potential energy curves involved in the cascade model of photodesorption of O^+ from O_2 adsorbed on Si(111) 7 × 7. V_{CH} is the neutral core excited state, V_{VH1} and V_{VH2} are valence hole excited states and V_N is the ground state [51].

phenomenon is believed to be due to the reduced number of free charge carriers (electrons) at low temperature. This is expected to affect preferentially the slower processes (low kinetic energy of desorbed species), thus explaining the reduced relative intensity of the 4 eV band in figure 10.

These results demonstrate that ion desorption mechanisms may be very complex. The MGR model provides a general understanding of ion desorption. However, the ion KED measurements have shown that simplified models cannot account for the experimental observations, in particular the isotope and temperature effects. More sophisticated models involving cascade transitions between ionic states need to be considered, i.e. the dynamics of ion PSD does not occur on a single ionic state but successively on several ionic states, each of them having a different relaxation lifetime.

8. Conclusion

We have shown that ion PSD enables a large variety of processes to be investigated, related to the adsorption of molecules on silicon surfaces and the molecular dynamics following their electronic excitation. Examples have been given of the adsorption configurations of O_2 on Si(111) 7 × 7, the physisorption–chemisorption transition of benzene molecules on Si(111) 7 × 7, the ion PSD of methanol adsorbed on Si(111) 7 × 7 compared to the fragmentation of gas phase methanol, the comparison between ion PSD of formic acid adsorbed on the Si(111) 7 × 7 and Si(100) 2 × 1 surfaces, the chemical selectivity of ion PSD following core level excitation of dissociatively adsorbed NO on Si(111) 7 × 7 and the detailed mechanisms of O^+ ion PSD from O_2 on Si(111) 7 × 7.

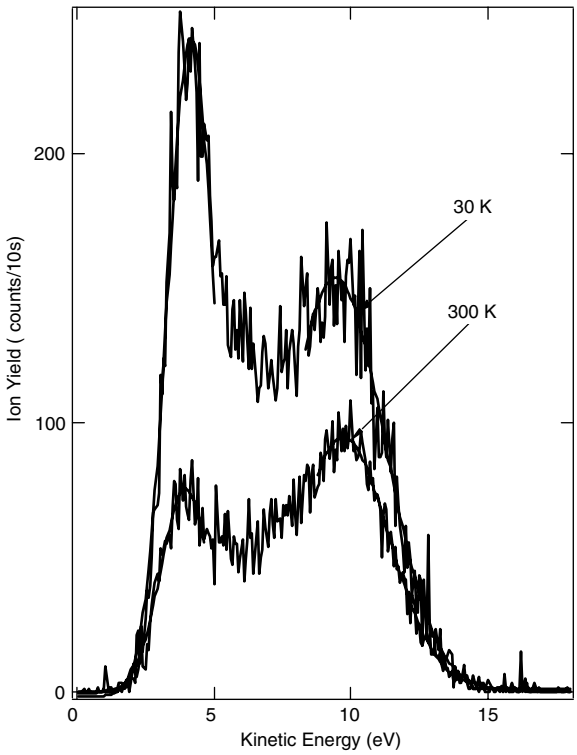

Figure 10. O^+ photoion KED after a 1.35 L O_2 exposure on the Si(111) 7 × 7 surface at 300 K (a) and after a 0.25 L O_2 exposure on the Si(111) 7 × 7 at 30 K (b). The photon energy is 108 eV [50].

Ion PSD has two main advantages compared to other surface techniques. First, it provides information on both the structure of the adsorbed molecules and the molecular dynamics after electronic excitation. Second, since ion PSD has a high surface sensitivity, the analysis of the experimental results does not require the subtraction of any process associated with the bulk substrate. The main disadvantage of ion PSD is that its sensitivity decreases as the mass of the desorbed ions increases. This limits the investigation to the desorption of low mass ions.

So far, ion PSD has been used as a probe to investigate surface processes. This implied that the photon illumination was low enough to avoid any substantial photon induced surface modification. With the advent of third generation synchrotron radiation (SR) sources, the photon brightness has now increased by several orders of magnitude. Neutral and ion PSD is becoming a severe problem for any surface study using these SR sources and the surface is going to be significantly modified. However, this can be turned into an advantage when using the SR as a tool for modifying in a controlled manner the surface structure and reactivity. Preliminary studies in this direction have been performed with a second generation SR source by using the zero order of the monochromator [63–65]. A hydrogenated Si(100) 2 × 1 surface has been progressively dehydrogenated, by being exposed to the unmonochromatized SR (from the visible range to about 250 eV) from 10 min up to 2 h. Two specific surface states have been discovered [63]. Similarly, a hydrogenated diamond surface has been partially dehydrogenated after exposure to the unmonochromatized ($h\nu = 150$–600 eV) synchrotron radiation for up to 2 h [64]. New and specific adsorption sites were created, which have been shown to react with oxygen molecules [65].

Finally, we wish to mention that all the information obtained by ion PSD on the adsorption of molecules on semiconductor surfaces and the molecular dynamics following their electronic excitation is valuable to the development of further surface studies, in particular the atomic scale manipulation of individual molecules with the scanning tunnelling microscope [66].

Acknowledgments

We are grateful to L Hellner, M Carbone, K Bobrov and A Hoffmann for invaluable help.

References

[1] Joachim C, Gimzewski J K and Aviram A 2000 *Nature* **408** 541
[2] Burroughes J H, Bradley D D C, Brown A R and Marks R N 1990 *Nature* **347** 359
[3] Forrest S R 1997 *Chem. Rev.* **97** 1793
[4] Brïtting W, Berleb S and Mückl A 2001 *Org. Electron.* **2** 1
[5] Katz H E 1997 *J. Mater. Chem.* **7** 369
[6] Horowitz G 1998 *Adv. Mater.* **10** 365
[7] Yi J W, Lee Y H and Farouk B 1998 *Thin Solid Films* **326** 154
[8] Comtet G, Dujardin G, Hellner L and Petravic M 2002 *Photonic, Electronic and Atomic Collisions* ed J Burgdörfer *et al* (Paramus, NJ: Rinton Press) p 93
[9] Fadley C S *et al* 1997 *Prog. Surf. Sci.* **54** 341
[10] Stöhr J 1996 *NEXAFS Spectroscopy* (*Springer Series in Surface Sciences*) ed G Ertl, R Gomer, L Douglas and L Mills (Berlin: Springer)
[11] Knotek M L, Jones V O and Rehn V 1979 *Phys. Rev. Lett.* **43** 300
[12] Madey T E, Stockbauer R L, Eastman D E and van der Veen J F 1980 *Phys. Rev. Lett.* **45** 187
[13] Madey T E 1994 *Surf. Sci.* **299/300** 824
[14] Feulner P, Treichler R and Menzel D 1981 *Phys. Rev.* B **24** 7427
[15] Yarmoff J A, Taleb-Ibrahimi A, McFeely F R and Avouris Ph 1988 *Phys. Rev. Lett.* **60** 960
[16] Ikeura H, Sekiguchi T, Tanaka K, Obi K, Ueno N and Honma K 1993 *Japan. J. Appl. Phys.* **32** 246
[17] Sekiguchi T, Ikeura H, Tanaka K and Obi K 1996 *J. Electron Spectrosc. Relat. Phenom.* **80** 65
[18] Sekiguchi H I and Sikiguchi T 1997 *Surf. Sci.* **390** 214
[19] Sekiguchi I and Sekiguchi T 1999 *Surf. Sci.* **435** 549
[20] Mase K, Nagasono M and Tanaka S 1999 *J. Electron Spectrosc. Relat. Phenom.* **103** 13
[21] Mase K, Tanaka S, Nagaoka S and Urisu T 2000 *Surf. Sci.* **451** 143
[22] Sekiguchi T, Ikeura-Sekiguchi H and Baba Y 2000 *Surf. Sci.* **454** 363
[23] Baba Y, Wu G, Sekiguchi T and Shimoyama I 2001 *J. Vac. Sci. Technol.* **19** 1485
[24] Sekitani T, Ikenaga E, Fujii K, Mase K, Ueno N and Tanaka K 1999 *J. Electron Spectrosc. Relat. Phenom.* **103** 135
[25] Nagaoka S, Tanaka S and Mase K 2001 *J. Phys. Chem.* **105** 1554
[26] Kizaki H, Wada S, Sako E O, Sumii R, Waki S, Isari K, Sekitani T, Sekiguchi T and Tanaka K 2005 *J. Electron Spectrosc. Relat. Phenom.* **144** 447
[27] Okudaira K K, Kobayashi E, Kera S, Mase K and Ueno N 2005 *Surf. Sci.* **593** 297
[28] Ikenaga E, Kudara K, Kusaba K, Isari K, Sardar S A, Wada S, Mase K, Sekitani T and Tanaka K 2001 *J. Electron Spectrosc. Relat. Phenom.* **114** 585
[29] Sekiguchi T, Sekiguchi H I and Tanaka K 1997 *Surf. Sci.* **390** 1
[30] Ikenaga E, Isari K, Kudara K, Yasui Y, Sardar S A, Wada S, Sekitani T, Tanaka K, Mase K and Tanaka S 2001 *J. Chem. Phys.* **114** 2751
[31] Wada S, Sumii R, Isari K, Waki S, Sako EO, Sekiguchi T, Sekitani T and Tanaka K 2003 *Surf. Sci.* **528** 242
[32] Okudaira K K, Watanabe T, Kera S, Kobayashi E, Mase K and Ueno N 2005 *J. Electron Spectrosc. Relat. Phenom.* **144** 461
[33] Tanaka K, Tinone M C K, Ikeura H, Sikiguchi T and Sekitani T 1995 *Rev. Sci. Instrum.* **66** 1474
[34] Mase K, Nagasono N, Tanaka S, Kamada M, Urisu T and Murata Y 1997 *Rev. Sci. Instrum.* **68** 1703
[35] Kato K, Uda T and Terakura K 1998 *Phys. Rev. Lett.* **80** 2000
[36] Nakajima K, Okazaki Y and Kimura K 2001 *Phys. Rev.* B **63** 113314
[37] Estève A, Chabal Y J, Raghavachari K, Weldon M K, Queeney K T and Rouhani M D 2001 *J. Appl. Phys.* **90** 86102

[38] Dujardin G, Comtet G, Hellner L, Hirayama T, Rose M, Philippe L and Ramage M J 1994 *Phys. Rev. Lett.* **73** 1727
[39] Comtet G, Dujardin G, Hellner L and Mayne A 1996 *Europhys. Lett.* **36** 355
[40] Comtet G, Hellner L, Dujardin G and Bobrov K 2002 *Phys. Rev.* B **65** 035315
[41] Carbone M, Zanoni R, Piancastelli M N, Comtet G, Dujardin G and Hellner L 1996 *Surf. Sci.* **352–354** 391
[42] Carbone M, Piancastelli M N, Zanoni R, Comtet G, Dujardin G and Hellner L 1997 *Surf. Sci. Lett.* **370** L179
[43] Carbone M, Piancastelli M N, Zanoni R, Comtet G, Dujardin G and Hellner L 1997 *Surf. Sci.* **390** 219
[44] Carbone M, Piancastelli M N, Casaletto M P, Zanoni R, Comtet G, Dujardin G and Hellner L 2003 *Chem. Phys.* **289** 93
[45] Carbone M, Piancastelli M N, Casaletto M P, Zanoni R, Comtet G, Dujardin G and Hellner L 2000 *Phys. Rev.* B **61** 8531
[46] Carbone M, Piancastelli M N, Casaletto M P, Zanoni R, Besnard-Ramage M J, Comtet G, Dujardin G and Hellner L 2003 *J. Phys.: Condens. Matter* **15** L327
[47] Hoffman A, Comtet G, Hellner L, Dujardin G and Petravic M 1998 *Appl. Phys. Lett.* **73** 1152
[48] Hoffman A, Petravic M, Comtet G, Heurtel A, Hellner L and Dujardin G 1999 *Phys. Rev.* B **59** 3203
[49] Hellner L, Comtet G, Ramage M J, Bobrov K, Carbone M and Dujardin G 2003 *J. Chem. Phys.* **119** 515
[50] Comtet G, Dujardin G and Hellner L 2003 *Surf. Sci.* **528** 210
[51] Comtet G and Dujardin G 2005 *Surf. Sci.* **593** 256
[52] Sakamoto K, Doi S, Ushimi Y and Ohtno K 1999 *Phys. Rev.* B **60** R8464
[53] Matsui F, Yeom H W, Amemiya K, Tono K and Ohta T 2000 *Phys. Rev. Lett.* **85** 630
[54] Hoshino T and Nishioka Y 2000 *Phys. Rev.* B **61** 4705
[55] Lee S H and Kang M H 2000 *Phys. Rev. Lett.* **84** 1724
[56] Aziza M, Baptist E, Brenac A, Chauvet G and Nguyen Tan T A 1987 *J. Physique* **48** 81
[57] Comtet G, Bobrov K, Hellner L and Dujardin G 2004 *Phys. Rev.* B **69** 155315
[58] Carbone M, Bobrov K, Comtet G, Dujardin G and Hellner L 2000 *Surf. Sci* **467** 49
[59] Tanaka S, Onchi M and Nishijima M 1989 *J. Chem. Phys.* **91** 2712
[60] Ikeura-Sekiguchi H, Sekiguchi T and Tanaka K 1999 *Phys. Rev.* B **53** 12655
[61] Carbone M, Piancastelli M N, Zanoni R, Comtet G, Dujardin G and Hellner L 1998 *Surf. Sci.* **407** 275
[62] Feulner P and Menzel D 1995 Electronically stimulated desorption of neutrals and ions from adsorbed and condensed layers *Laser Spectroscopy and Photochemistry on Metal Surfaces* (*Advanced Series in Physical Chemistry* vol 5) ed H-L Dai and W Ho (Singapore: World Scientific) and references therein
[63] Bobrov K, Comtet G, Dujardin G and Hellner L 2001 *Phys. Rev. Lett.* **86** 2633
[64] Bobrov K, Comtet G, Dujardin G, Hellner L, Bergonzo P and Mer C 2002 *Phys. Rev.* B **65** 035315
[65] Bobrov K, Comtet G, Hellner L and Dujardin G 2004 *Appl. Phys. Lett.* **85** 296
[66] Comtet G, Dujardin G, Hellner L, Lastapis M, Martin M, Mayne A J and Riedel D 2004 *Phil. Trans. R. Soc.* A **362** 1217